THE PENNSYLVANIA STATE UNIVERSITY
SCHREYER HONORS COLLEGE

DEPARTMENT OF CHEMICAL ENGINEERING

AN ANALYSIS OF PROTEIN ADSORPTION AND DESORPTION FROM ANION EXCHANGE RESINS WITH APPLICATIONS TO COUNTERCURRENT TANGENTIAL CHROMATOGRAPHY

MORGAN BARTH

Spring 2010

A thesis
submitted in partial fulfillment
of the requirements
for a baccalaureate degree
in Chemical Engineering
with honors in Chemical Engineering

Reviewed and approved* by the following

Andrew Zydney
Department Head
Walter L. Robb Chair & Professor of Chemical Engineering
Thesis Supervisor

Themis Matsoukas
Professor, Chemical Engineering
Honors advisor

*Signatures are on file in the Schreyer Honors College

Abstract

Column chromatography is used extensively for the purification of high value biological products, exploiting differences in binding affinity to achieve high resolution separations. There are significant challenges in using packed bed chromatography columns for very large scale processes including: poor flow distribution, excessive pressure drops, column packing issues, slow operation, and high cost. Countercurrent tangential chromatography has recently been proposed as an alternative separation process, with the chromatography resin pumped in the form of a slurry through multiple hollow fiber membrane modules using a countercurrent configuration. The objective of this thesis was to obtain quantitative data for the rates of protein adsorption and desorption and binding equilibria on different anion exchange resins which are needed to design successful countercurrent chromatography systems.

Experiments were performed using two commercially available anion exchange resins, Macroprep 25Q and Q Sepharose, with bovine serum albumin (BSA) and myoglobin as model proteins. Data were obtained for protein adsorption and desorption as a function of time over a range of protein concentrations and resin volume fractions. The equilibrium binding data were in good agreement with a classical Langmuir isotherm with a maximum capacity for BSA of approximately 13 g/L for the Macroprep 25Q and 35 g/L for the Q Sepharose resin. The rate of adsorption was described using a simple mass transfer model with a lumped mass transfer coefficient. Uptake kinetics were much faster with Macroprep 25Q than Q Sepharose due to its smaller particle size. These results provide important information that can be used for the design of effective countercurrent tangential chromatography systems.

Table of Contents

List of Figures and Table

1. Introduction

1.1. Principles of Chromatography

Liquid chromatography is one of the most powerful and widely used tools for the purification of biological molecules. The feed solution, or mobile phase, is typically pumped through a cylindrical column packed with solid particles, also referred to as the stationary phase or resin. Separation occurs because of interactions between the product (and impurities) and the solid phase. For example, in anion exchange chromatography a positively-charged resin can be used to bind (and thus purify) a negatively-charged product while allowing weakly charged impurities to pass through the column. Highly specific binding interactions are exploited in affinity chromatography, e.g., the use of Protein A to capture a monoclonal antibody. The most common mode of operation is typically referred to as bind-and-elute chromatography, in which the desired product is first bound by the stationary phase while impurities are washed away. The product is then eluted from the column by changing the buffer conditions to reverse the interactions so that the product can be collected in the liquid phase. Additional information about the use of chromatography for protein purification is provided in references [1] – [4].

This thesis focuses on the use of ion exchange resins for protein purification. A typical ion exchange resin consists of porous polymer particles (beads) modified with fixed charge groups. Common polymers used to make ion exchange resins are styrene-divinyl-benzene, acrylates, methylacrylates, polyamines, cellulose, and dextran [5]. The charge groups include sulfonyl (pK = 1), carboxyl (pK = 4), diethylaminoethyl (pK = 10), and quaternary ethylamine (pK = 14). Sulfonyl and quaternary ethylamine resins are

strong acids and bases, respectively, with binding capacities that are largely independent of solution pH [6].

Figure 1 provides a schematic showing the mechanism of adsorption in ion exchange chromatography. The fixed charges on the positively charged resin, seen in the upper part of the picture, are initially associated with negative counter-ions to preserve the overall electrical neutrality of the system. The negatively-charged protein binds more strongly to the charged resin, displacing multiple counter-ions from the surface. Impurities can thus be washed away from the product using an appropriate wash buffer.

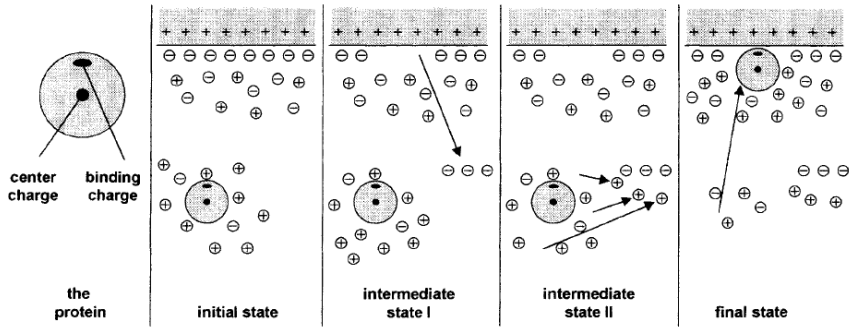

Figure 1: Model of adsorption of a negatively charged protein by a positively charged resin. Taken from [7].

1.2. Limitations of Packed Bed Chromatography

Chromatography is used in the downstream processing of essentially all biologic products produced by recombinant gene technology. These biotechnology drugs are used to treat a variety of infectious diseases, cancers, and autoimmune deficiencies. These products make up a quarter of new FDA filings and account for over 40% of current preclinical trials [8].

Recent improvements in cell culture technology have increased product titers by as much as a factor of 5 in just the last 5-10 years. This has placed increased demands on the downstream purification technology since the required resin volume is determined by

the mass of product that must be recovered from the cell culture fluid. In order to scale up chromatography columns to accommodate these increased product titers, the cross-sectional area of the column must be increased; increasing the bed height is typically not an option because of the excessive pressures required to drive the fluid through the packed column [9]. The maximum bed diameter for current commercial columns is 2 m; thus, further increases in capacity must be accommodated by using multiple columns in parallel or by using a single column with multiple cycles.

In addition to capacity limitations, chromatography is often one of the more expensive components in the overall cost of manufacturing therapeutic proteins. The detailed costs are dependent on the specific properties of the product and the targeted production rate, but approximately 80% of the cost for producing 100 kg/yr of a typical monoclonal antibody is associated with the downstream processing, with the largest component being the cost of the Protein A used in the first chromatography step. For example, a 10,000 L bioreactor producing a monoclonal antibody at a concentration of approximately 1 g/L would require a Protein A column that would cost $4-5 million [10]. Even greater costs would be incurred in the future based on the recent increases in product titer.

1.3. Countercurrent Tangential Chromatography

One possible approach for overcoming many of the limitations of packed bed columns is to use countercurrent tangential chromatography, a newly patented process for the large scale purification of high value biological products [11]. In countercurrent tangential chromatography, the binding interactions between the product and resin occur

in suspension, instead of in a packed column, with the washing and elution steps accomplished using tangential flow hollow fiber membrane modules that retain the resin particles while allowing the surrounding fluid to pass through the membrane pores. The system is arranged with countercurrent flow of the slurry and buffer, significantly improving process efficiency and reducing the required buffer volumes.

Countercurrent chromatography can be performed in either batch or continuous mode. In the batch mode, the individual chromatography steps (binding, washing, elution, regeneration, and equilibration) are performed separately. For example in the elution step, the slurry (initially containing the bound product) would be mixed with elution buffer and then pumped through two hollow fiber modules, with the permeate stream from the second module mixing with the slurry flow at the inlet to the first module. This is shown schematically in Figure 2. The system consists of two static mixers (102 & 106) and two hollow fiber modules (104 & 108) in series. The resin slurry enters through the first input port (101) while the buffer (or unpurified product for the binding step) enters the second static mixer through the second input port (107). The permeate from the second filter is recycled back to the first static mixer (103) while the permeate from the first filter is discarded as waste (in binding, washing, regeneration, and equilibration) or collected as a product (in elution).

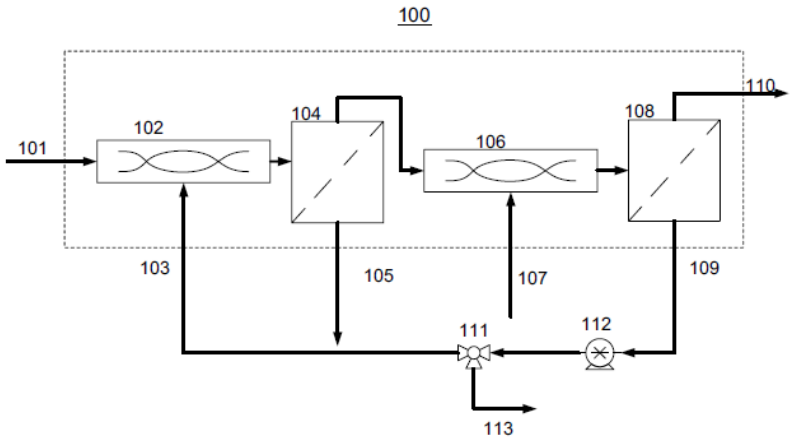

Figure 2: Schematic of hollow fiber modules and static mixers in countercurrent tangential flow chromatography. Taken from [11].

In continuous operation, countercurrent tangential chromatography would employ multiple hollow fiber modules connected in "stages" to enable binding, washing, elution, and regeneration all to occur in series as the slurry flows through the system. Thus, the first stage would be used to bind the product, with the resin (containing the bound product) immediately pumped through the washing stage and then into the elution stage, using appropriate buffers in the different stages. This significantly reduces the amount of resin needed to purify the feed stream since essentially the entire resin is in use at all times [11]. Countercurrent tangential chromatography has enormous potential to overcome the capacity limitations found with current packed bed columns while also providing opportunities for the design of relatively low-cost disposable systems that would eliminate issues associated with column packing, cleaning, and validation.

One of the challenges in designing an effective countercurrent tangential chromatography system is providing sufficient contacting time in the binding and elution steps to ensure complete (or nearly complete) recovery of the high value product. The

system shown in Figure 2 uses static mixers before each hollow fiber membrane module, with the volume of the static mixer chosen to provide sufficient residence time for essentially complete binding (or elution). Proper design of the static mixers requires accurate and quantitative data for the intrinsic adsorption (binding) and desorption kinetics, while the equilibrium binding isotherm is needed to determine the amount of resin required to effectively recover a given product from the feed mixture.

The objective of the work described in this thesis was to obtain quantitative data for binding kinetics and equilibrium for two commercially available ion exchange resins using bovine serum albumin as a model product. Data were analyzed using simple binding models (described in Chapter 2), with the resulting rate constants and equilibrium binding parameters providing the information needed to design and demonstrate the feasibility of a countercurrent tangential chromatography system.

2. Binding Models

2.1. Adsorption Equilibrium

One of the simplest approaches for analyzing the adsorption equilibrium for chromatography resins is to use the Langmuir adsorption isotherm. This model is developed by assuming that proteins adsorb (or bind) to a fixed number of sites on the solid, all of which are assumed to be energetically equivalent, and that there are no interactions between adsorbed molecules [12]. The model also assumes reversible equilibrium between the protein in free solution (P) and the bound protein (P*):

$$\mathrm{P} + * \leftrightarrow \mathrm{P}* \tag{1}$$

where the open adsorption site is denoted by *. The rates of adsorption and desorption are assumed to be proportional to the concentrations of protein, free adsorption sites, and adsorbed protein:

$$\mathrm{r}_{ads} = k_a[\mathrm{P}][*] \tag{2}$$

$$\mathrm{r}_{des} = k_d[P*] \tag{3}$$

At equilibrium the rates of adsorption and desorption are equal with the equilibrium constant, $\mathrm{K_A}$ given as:

$$\mathrm{K_A} = \frac{k_a}{k_d} = \frac{[\mathrm{P}*]}{[\mathrm{P}][*]} \tag{4}$$

In order to put Equation (4) in a more convenient form, the concentration of open adsorption sites is expressed in terms of the total number of adsorption sites, $\mathrm{N_{tot}}$:

$$\mathrm{N_{tot}} = [*] + [\mathrm{P}*] = [*] + \mathrm{K_A}[\mathrm{P}][*] \tag{5}$$

Equation (5) can be directly solved for the concentration of free adsorption sites:

$$[*] = \frac{N_{tot}}{1 + K_A[P]} \tag{6}$$

Equation (6) can be inserted into the equilibrium expression, leading to the following expression for the concentration of adsorbed protein (in units of protein mass per volume solid) in terms of the free protein concentration (in units of protein mass per volume liquid):

$$[P*] = \frac{K_A N_{tot}[P]}{1 + K_A[P]} \tag{7}$$

At high protein concentrations, the amount of adsorbed protein approaches its maximum asymptotic value, which is equal to the total number of adsorption sites. At low protein concentrations, the amount of adsorbed protein varies linearly with the concentration of protein in the liquid phase:

$$[P*] = K_A N_{tot}[P] \tag{8}$$

Equation (7) can be placed in a more general linearized form as:

$$\frac{[P]}{[P*]} = \frac{[P]}{N_{tot}} + \frac{1}{K_A N_{tot}} \tag{9}$$

Thus a plot of the ratio of the protein concentration in the liquid phase to the concentration of adsorbed protein as a function of the protein concentration in the liquid phase should be linear with a slope equal to the reciprocal of the product of the total number of adsorption sites and the equilibrium constant.

Although Equation (7) provides an adequate description of protein adsorption on a variety of different solid phases, a number of alternative models have also been developed to describe equilibrium protein binding. One of the more successful of these for ion exchange materials is the steric mass action (SMA) model. The SMA model

assumes that protein adsorption can be described by an exchange reaction occurring between the protein and a specific number of counter-ions initially associated with the charge groups on the resin:

$$C_a + \upsilon_a \bar{Q}_s \leftrightarrow Q_a + \upsilon_a C_s \quad (10)$$

where C_s is the salt concentration in the fluid, C_a is the free (un-bound) protein concentration, Q_a is the bound protein concentration and Q_s is the bound salt concentration where the overbar signifies the salt that is available for exchange with the protein (steric limitations). The coefficient υ_a describes the characteristic charge of the protein. The protein reacts with υ_a sites on the resin and displaces an equal number of monovalent counter-ions. If the counter-ions are not monovalent the number of counter-ions displaced can be determined based on the ratio of the valencies. The equilibrium constant for protein binding, K_a is defined as:

$$K_a = \left(\frac{Q_a}{C_a}\right)\left(\frac{C_s}{\bar{Q}_s}\right)^{\upsilon_a} \quad (11)$$

The amount of bound counter-ions available for adsorption is related to the concentration of adsorbed protein through the steric factor, σ_a, as:

$$\bar{Q}_s = Q_s - \sigma_a Q_a \quad (12)$$

The protein capacity is related to the total resin capacity, Λ, as follows:

$$\Lambda = \bar{Q}_s + (\upsilon_a + \sigma_a) Q_a \quad (13)$$

Substituting Equation (13) into the equilibrium expression and rearranging results in the following expression for the free protein concentration:

$$C_a = \left(\frac{Q_a}{K_a}\right)\left(\frac{C_s}{\Lambda - (\upsilon_a + \sigma_a) Q_a}\right)^{\upsilon_a} \quad (14)$$

At high protein concentrations, the concentration of adsorbed protein approaches the maximum protein capacity of the resin, Q_a^{max}:

$$\lim_{C_a \to \infty} Q_a = \frac{\square}{\sigma_a + \upsilon_a} = Q_a^{max} \quad (15)$$

The expression for the protein concentration in the liquid can be rewritten in terms of the maximum protein capacity of the resin as:

$$C_a = \frac{Q_a}{K_a}\left(\frac{C_s}{Q_a^{max} - Q_a}\right)^{\upsilon_a} \quad (16)$$

Equation (16) can be linearized by taking the natural log of both sides of the equation and rearranging as follows:

$$\ln\left(\frac{C_a}{Q_a}\right) = -\upsilon_a \ln(Q_a^{max} - Q_a) + (\upsilon_a \ln C_s - \ln K_a) \quad (17)$$

A plot of the natural log of the ratio of the liquid protein concentration over the bound protein concentration versus the natural log of the difference between the maximum protein capacity and the equilibrium bound protein concentration gives a linear plot with a slope equal to the negative of the characteristic charge.

2.2. Adsorption and Desorption Kinetics

As discussed in Chapter 1, the rates of adsorption and desorption play a critical role in designing an effective countercurrent tangential chromatography system. In general, the observed rate of adsorption (or desorption) will be determined by the intrinsic binding kinetics, the rate of protein mass transfer from the bulk solution to the particle surface (external mass transport limitations), and the rate of protein diffusion within the porous resin particle (internal mass transport limitations).

The governing mass balances describing the adsorption and desorption processes can be written as:

$$\frac{dm_{p,s}}{dt} = \mathrm{V_s}\frac{d[P*]}{dt} = \dot{r} \quad (18)$$

$$\frac{dm_{p,l}}{dt} = \mathrm{V_L}\frac{d[P]}{dt} = -\dot{r} \qquad (19)$$

The volume of the liquid (V_L) and the resin (V_s) both remain constant during the adsorption / desorption experiments described in the next Chapter.

In order to solve Equations (18) and (19), we need to develop an expression for the rate of adsorption (r) in terms of the protein concentrations in the solid and liquid phases. The simplest approach is to assume that the rate is linearly proportional to the difference between the protein concentration in the liquid, [P], and the protein concentration that would be in equilibrium with the solid-phase concentration, $[P]_{eq}$ so that:

$$\dot{r} = k([P] - [P]_{eq}) \qquad (20)$$

The protein concentration that would be in equilibrium with the solid-phase concentration can be evaluated from the equilibrium isotherm, which for the Langmuir isotherm becomes:

$$[P]_{eq} = \frac{1}{K_A[*]_0}\left(\frac{1}{[P*]} - \frac{1}{[*]_0}\right)^{-1} \qquad (21)$$

Equations (18) to (21) can be used to describe the kinetics for both adsorption and desorption. In the case of desorption, the protein concentration in the liquid is less than the concentration that would be in equilibrium with the solid-phase concentration leading to a negative rate of adsorption. The methodology used to solve Equations (18) to (21) is described in Chapter 4.

3. Materials and Methods

3.1. Buffer and Resin Preparation

All adsorption experiments were performed using proteins dissolved in 20 mM phosphate buffer (PBS) at pH 7. PBS was prepared by dissolving appropriate amounts of sodium phosphate dibasic heptahydrate (4.0195 g) (J.T. Baker) and potassium phosphate monobasic crystal (2.089 g) (J.T. Baker) in deionized water (3.5 L) obtained from a NANOpure Diamond water purification system (Barnstead Thermolyne Corp). 0.1 M HCl or NaOH was added as needed to obtain a pH of 7.0 ± 0.1, with the pH evaluated using a Thermo Orion model 420Aplus pH meter. Bovine serum albumin (A7906) and myoglobin (M0630) were purchased from Sigma Aldrich and used as model proteins. Desorption experiments were performed using PBS containing added sodium chloride (J. T. Baker) to reduce the strength of the electrostatic interactions.

Binding experiments were performed with Q Sepharose and Macroprep 25Q, both strong anion exchange resins. The Q Sepharose is made with a matrix of cross-linked agarose and modified with a quaternary amine functionality ($N^+(CH_3)_3$). The Q Sepharose was in the form of spherical beads, ranging from 45 – 165 μm in diameter, with an average particle size of 90 μm [14]. The Macroprep 25Q has a much smaller average particle size of approximately 25 μm and is made with a more rigid methacrylate base again modified with a quaternary amine functionality [15].

Both resins were stored in 20% ethanol to minimize bacterial growth during long term storage. The resins were placed in the desired operating buffer by performing several buffer exchanges using a 200 mL ultrafiltration cell fitted with a 0.45 μm HV Durapore membrane (HVP09050, Millipore Corporation). Approximately 40 mL of the

slurry (with particle volume fraction of 70%) was allowed to settle in the stirred cell. The resin was then washed with PBS using 3-4 times the original suspension volume. Filtration was performed at a pressure of approximately 7 psi in the absence of any stirring. The slurry was then carefully removed from the ultrafiltration cell, poured into a 100 mL graduated cylinder, and allowed to settle overnight. The particle concentration in the slurry (volume particles per total volume of slurry) was determined from the ratio of the height of the sedimented particle layer to the total height in the graduated cylinder. Note that this does not account for the trapped fluid volume within the sedimented slurry. Thus, the actual particle volume fraction will be approximately 70% of the value reported in this thesis. The actual particle volume fraction was used in all calculations and analysis.

3.2. Adsorption and Desorption Experiments

Adsorption and desorption experiments were performed in a small stirred beaker with a total volume of 40 mL. For the adsorption experiments, protein was initially dissolved in 20 mM PBS containing 6.25 mM NaCl. The beaker was initially filled with approximately 5 mL of the slurry. The stirrer was turned on at a low stirring speed and then 35 mL of the protein solution was rapidly added to the beaker. Small samples (approximately 0.6 mL) were collected through a syringe filter with a 0.2 μm pore size membrane that was fully retentive to the resin particles, allowing samples of the free solution to be obtained at specific times over the course of the experiment. Each syringe filter was used only once and then discarded. Experiments were performed over a range of slurry and protein concentrations as summarized in Table 1.

Table 1: Initial Concentrations of Resin and Protein Concentrations for Adsorption Experiments

10% Slurry	15% Slurry
0.5 g/L BSA	1.5 g/L BSA
1.0 g/L BSA	2.5 g/L BSA
1.5 g/L BSA	3.3 g/L BSA
2.0 g/L BSA	4.0 g/L BSA
2.5 g/L BSA	4.5 g/L BSA
0.285 g/L Myoglobin	

Desorption experiments were performed using slurries containing 10% or 15% resin that had initially been equilibrated for 30 min with a 1.5 g/L BSA solution in 20 mM PBS. The appropriate amounts of NaCl (200 or 300 mM NaCl) were rapidly added directly to the 40 mL slurry, with samples obtained through the syringe filter at specific times during the course of the experiment.

3.3. Sample Analysis

Samples were expelled from the syringe filter and placed into 96 well plates (using 200 μL per well), with the absorbance at 280 nm read using a UV spectrophotometer (Spectramax Plus 384). The BSA concentration was evaluated from a calibration curve constructed from data obtained with BSA samples of known concentration:

$$A_{280} = 0.2945[P] \tag{22}$$

as shown in Figure 3.

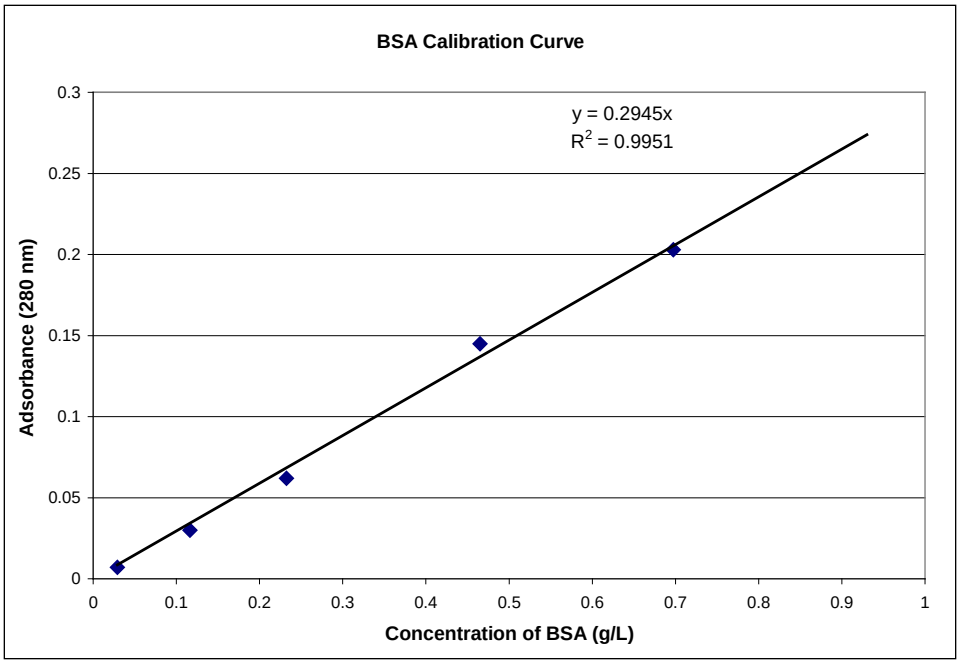

Figure 3: Calibration Curve Used to Evaluate the BSA Concentration

The myoglobin concentration was evaluated from a similar calibration curve constructed from data obtained with myoglobin samples of known concentration:

$$A_{280} = 0.6337[P] \tag{23}$$

4. Results and Analysis

4.1. BSA Adsorption

Typical experimental data for the BSA concentration in the liquid and solid phases as a function of time during a binding experiment using the Macroprep 25Q are shown in Figure 4. These data were obtained by mixing 6 mL of slurry having a resin concentration of 47% with 34 mL of a BSA solution with a concentration of 3.0 g/L. The initial BSA concentration in the liquid phase immediately after the addition can thus be estimated as 2.7 g/L assuming that the packed resin actually contains 70% solids. The BSA concentration in the liquid phase was evaluated directly from samples obtained through the syringe filter. The BSA concentration in the solid phase at each time point was determined from a simple mass balance as:

$$[P*] = \frac{[P]_0 V_L - [P] V_L}{V_r} \tag{24}$$

Where $[P]_0$ is the initial concentration of BSA. The total volume of liquid (V_L) was taken as a constant; the volume of all collected samples (approximately 3.5 mL) was less than 10% of the initial liquid volume. V_r is the volume of the resin, calculated directly from the slurry concentration.

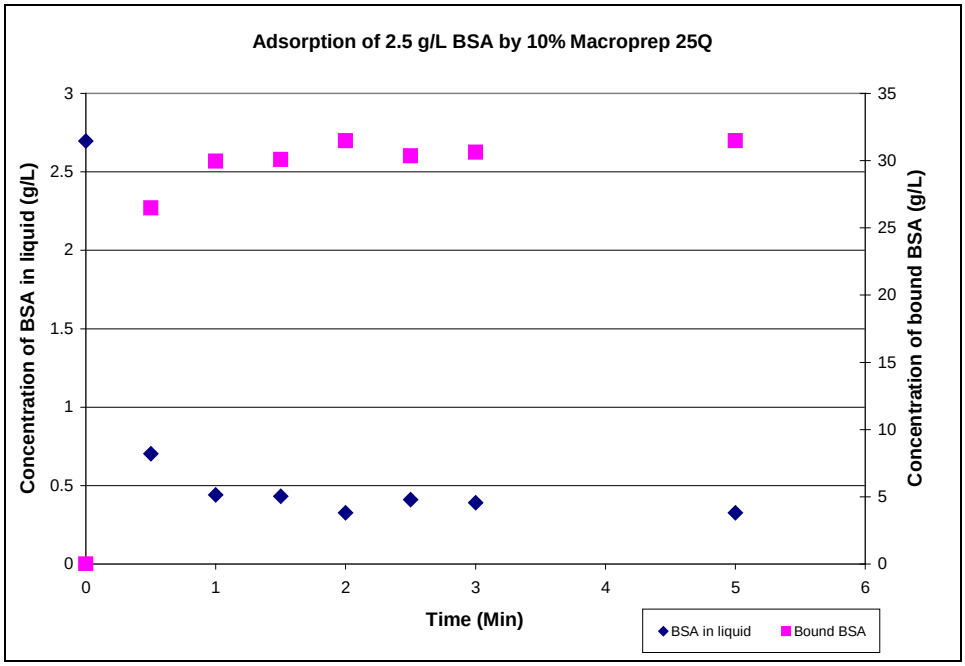

Figure 4: Concentration of BSA in the liquid and adsorbed to the solid for an adsorption experiment performed with 10% Macroprep 25Q and a 2.5 g/L BSA solution in 20 mM PBS, 6.25 mM NaCl, at pH 7

The BSA concentration in the liquid phase decreases with time as the protein binds to the resin. The binding kinetics are very fast with the BSA concentrations in both the liquid and solid phases becoming constant, independent of time, for t > 2 min. Further analysis of the binding kinetics is discusses in the next section. For the data in Figure 4, the equilibrium concentration of bound protein is approximately 100 times that in the liquid phase (note different axes in Figure 5), consistent with the strong electrostatic interactions between the negatively-charged BSA and the positively-charged resin.

4.2. Langmuir Isotherm

The data for the equilibrium binding for a series of experiments performed using the Macroprep 25Q resin are shown in Figure 5. The y-axis shows the concentration in the solid phase, calculated directly from the measured liquid-phase concentration at equilibrium using Equation (24). The equilibrium concentration of adsorbed BSA clearly approaches a maximum value, N_{tot}, at liquid-phase concentrations greater than about 0.2 g/L, reflecting the saturation of all binding sites on the resin.

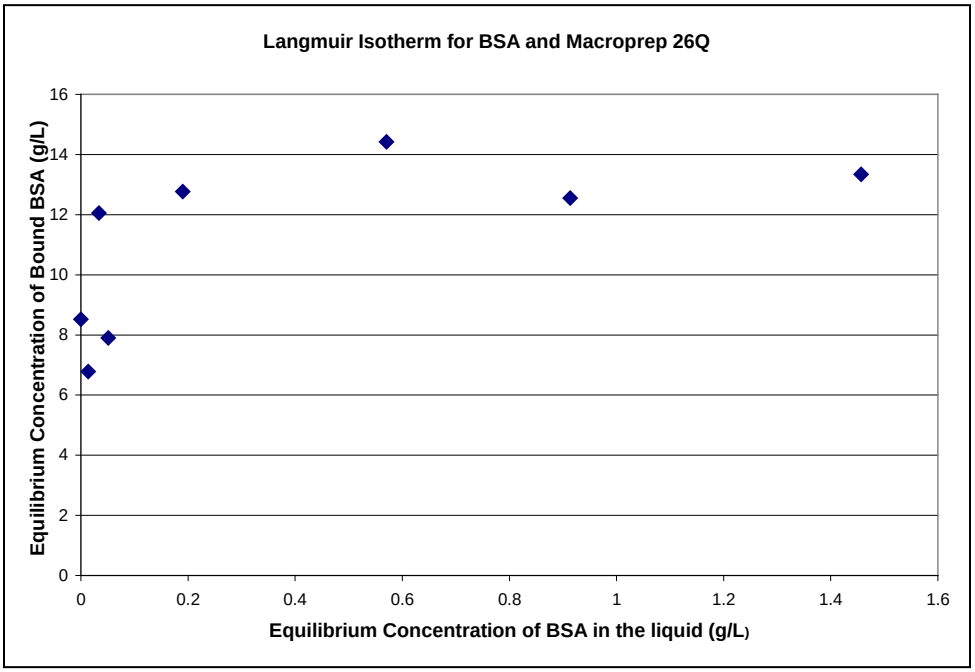

Figure 5: Equilibrium binding data for BSA to the Macroprep 25Q resin in 20 mM PBS, 6.25 mM NaCl, at pH 7.

The experimental data in Figure 5 have been re-plotted in Figure 6 using the linearized form of the Langmuir binding isotherm (Equation 9). The data are highly linear when plotted in this manner with an r^2 value greater than 0.99. The values of the

maximum resin capacity, N_{tot}, and the equilibrium binding constant, K_A, were calculated directly from the slope and intercepts as

$$N_{tot} = \frac{1}{m} \tag{25}$$

$$K_A = \frac{1}{bN_{tot}} \tag{26}$$

with the results summarized in Table 2. The equilibrium binding constant for the Macroprep 25Q was 11 L/g, indicating that binding saturation at BSA concentrations much about 0.3 g/L.

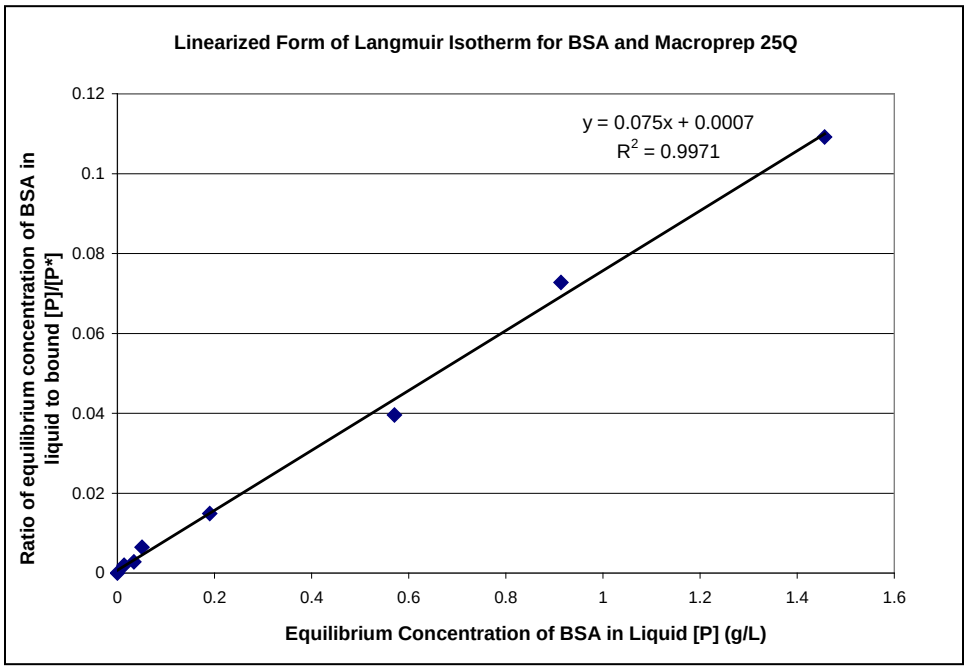

Figure 6: Experimental data for BSA binding to the Macroprep 25Q plotted using the linearized form of the Langmuir isotherm

Corresponding results for the Q Sepharose resin are shown in Figure 8. While the experimental results follow a similar trend to the results obtained with the Macroprep 25Q, the data are more scattered with $r^2 = 0.84$. The variability in the Q Sepharose data could be due to non-equilibrium effects associated with the short time (5 min) used in

these experiments. Figure 7 shows the experimental data for the adsorption of 3.3 g/L BSA by 15% Q Sepharose. In this graph it is difficult to prove that the liquid concentration of BSA has actually reached an equilibrium concentration within the first 5 minutes. The 5 min adsorption time was more than sufficient for the Macroprep 25Q given the rapid binding kinetics for that resin. However, the Q Sepharose has a significantly larger particle radius, which could lead to significant internal diffusional limitations during the binding experiments. There was insufficient time during the semester to directly evaluate the binding kinetics of BSA to the Q Sepharose resin.

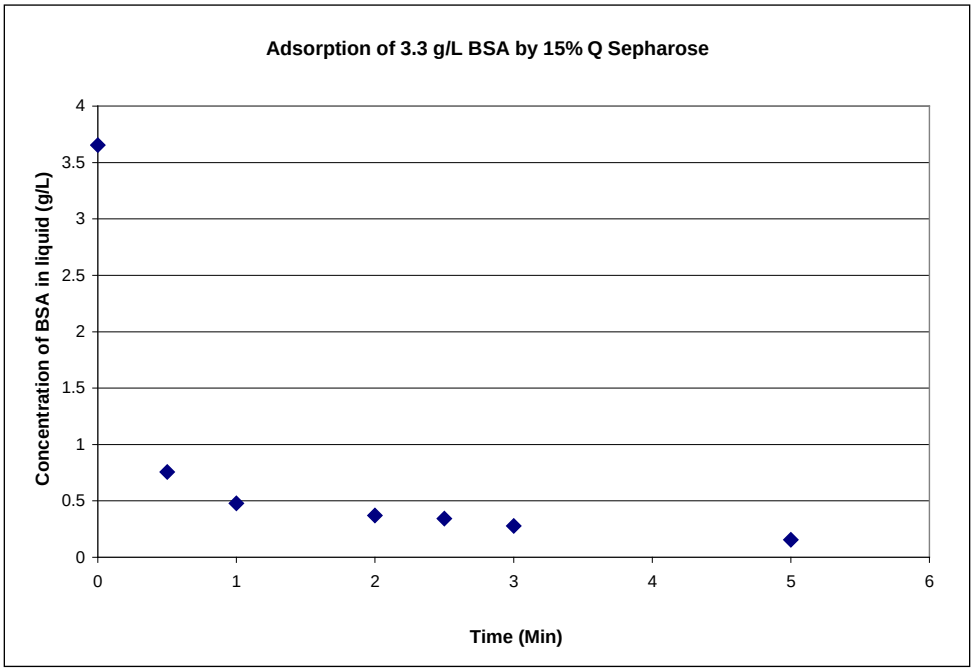

Figure 7: Adsorption kinetics for the Q Sepharose resin with 3.3 g/L solution of BSA in 20 mM PBS, 6.25 mM NaCl at pH 7

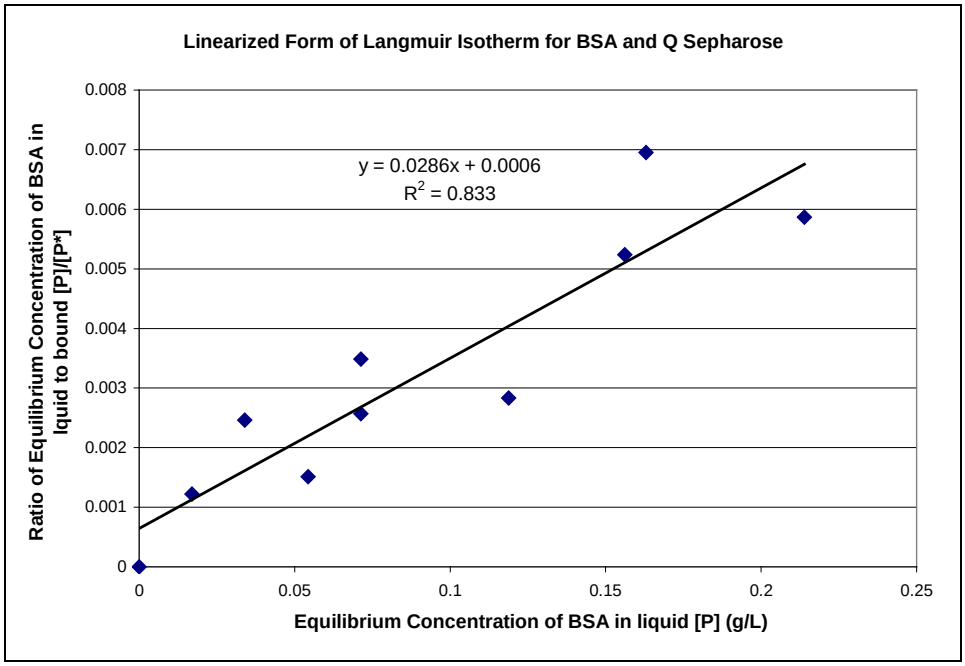

Figure 8: Experimental data for BSA binding to the Q Sepharose plotted using the linearized form of the Langmuir isotherm for experiments in 20 mM PBS, 6.25 mM NaCl, at pH 7

Table 2: Langmuir Binding Parameters for BSA Adsorption to the Macroprep 25Q and Q Sepharose Resins in 20 mM PBS, 6.25 mM NaCl at pH 7

	Slope (L/g)	**Intercept**	**Max Resin Capacity, N_{tot} (g/L)**	**Equilibrium Constant, K_A (L/g)**
Q Sepharose	0.0286	0.0006	35	5
Macroprep 25Q	0.075	0.007	13	11

The Langmuir isotherm parameters for the Q Sepharose resin were determined from the slope and intercept of the plot in Figure 8. The maximum binding capacity of the Q Sepharose resin is 35 g/L, which is 2.5 times the maximum capacity of the Macroprep 25Q (N_{tot} = 13 g/L). The maximum binding capacity is related to the internal surface area of the resin and the density of the ion exchange groups. According to the manufacturers, Q Sepharose has a maximum binding capacity for BSA of 120 g/L while

Macroprep 25Q has a maximum capacity of only 30 g/L, with this 4:1 ratio being even greater than that found in this work. In contrast, data obtained by Staby et al. gave an average maximum capacity of 21 g/L for Macroprep 25Q and 54 g/L for Q Sepharose, [16], with the ratio of the equilibrium capacities (2.6) in excellent agreement with the data reported in Chapter 2. The origin of these differences in the absolute values of the equilibrium binding capacities is unclear, although this could be due to small differences in the buffer conditions.

One possible source of error in the experimental determination of the equilibrium binding constants is the assumption of constant liquid volume throughout the experiment. A typical binding experiment involved taking 7 samples from the liquid solution giving a total volume change between 3 and 4 mL. The resulting changes in the liquid volume and the mass of BSA in these samples were not accounted for in the calculations. These changes would cause a shift in the equilibrium concentration of adsorbed BSA. However, the effect is too small to explain the discrepancies between the data obtained in this study and that reported by Staby et al.

4.3. Steric Mass Action Model

The adsorption equilibrium data were also analyzed using the Steric Mass Action (SMA) model given by Equation (17). An initial estimate of the maximum resin capacity was taken from Staby et al. A graph was then constructed of the natural log of the ratio of the protein concentration in the liquid to that bound to the resin as a function of the natural logarithm of the difference between the maximum protein capacity and the bound protein concentration with the results shown in Figure 9. The data are highly scattered

when plotted in this manner. The magnitude of the scatter could be reduced by adjusting the value of Q_a^{max}, although the resulting plots still had relatively low correlation coefficients. This suggests that the SMA model is inappropriate for describing BSA adsorption to the Macroprep 25Q, although additional experimental data over a broader range of conditions would be needed to verify this conclusion.

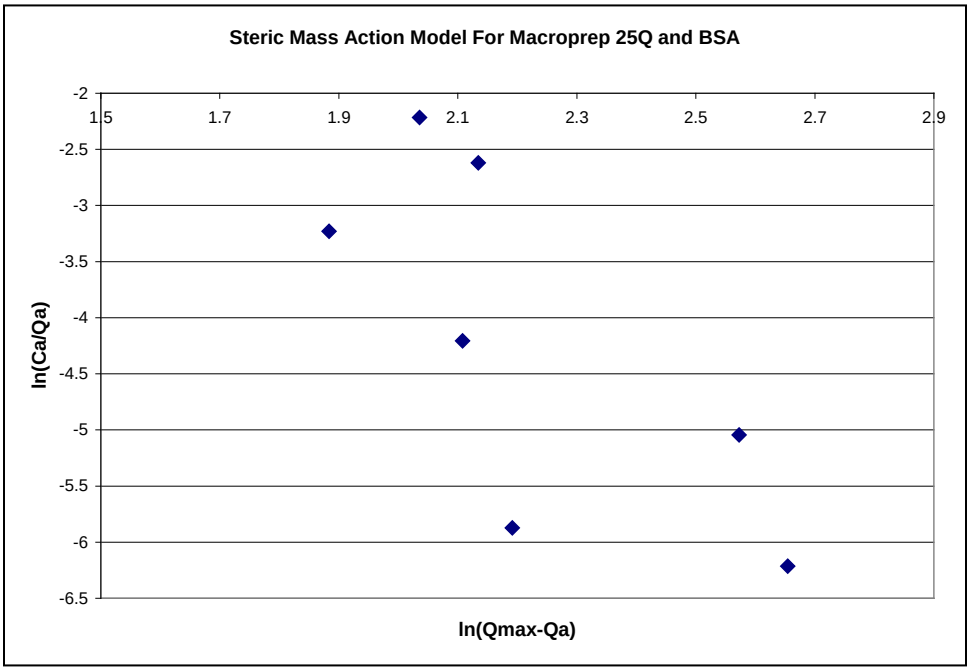

Figure 9: Equilibrium binding data for BSA to the Macroprep 25Q resin plotted using the linearized form of the Steric Mass Action model

4.4. Binding Kinetics

The adsorption kinetics for BSA binding to the Macroprep 25Q and the Q Sepharose resin are compared in Figure 10 for experiments performed with an initial BSA concentration of 2.5 g/L using a 10% slurry. In both cases, the BSA concentration in the liquid phase decreases by a factor of 5 within the first minute with very similar profiles during this initial phase. However, the liquid phase concentration in the

experiment performed with the Q Sepharose resin continues to decrease with time out until at least t = 5 min.

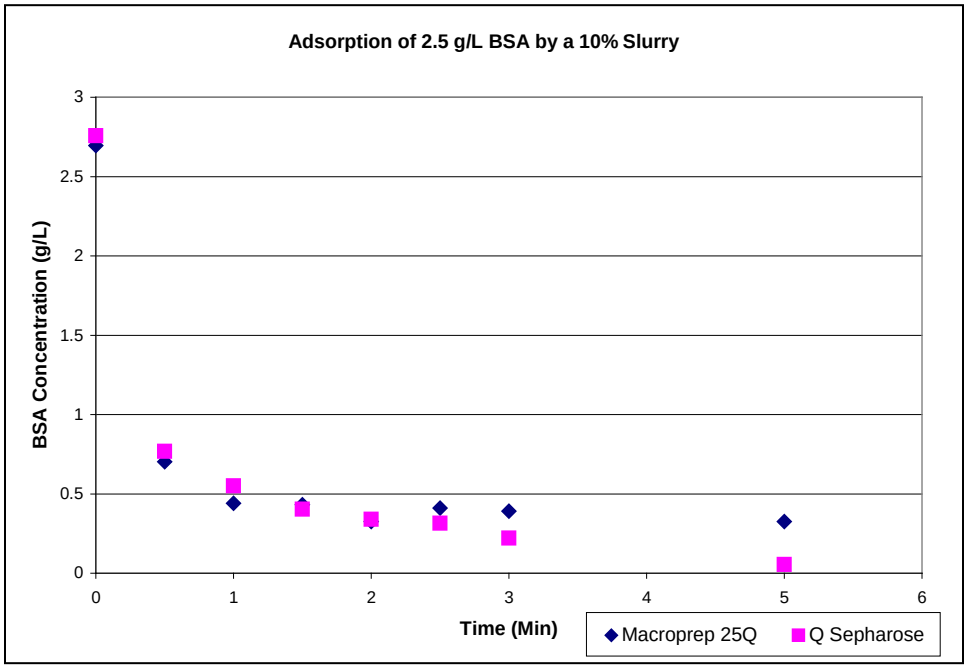

Figure 10: Adsorption kinetics for the Macroprep 25Q and the Q Sepharose resins for experiments with a 2.5 g/L solution of BSA in 20 mM PBS, 6.25 mM NaCl at pH 7

The experimental data were analyzed using the simple theoretical model presented in the Introduction. The mass balances were integrated numerically using a time step of 0.01 min, with the concentrations of BSA in the liquid, the solid, and in the liquid that would be in equilibrium with the solid evaluated at each time step as:

$$[P]_{i+1} = [P]_i - \frac{k([P]_i - [P]_{eq,i})}{V_L}(t_{i+1} - t_i) \quad (26)$$

$$[P*]_{i+1} = [P*]_i + \frac{k([P]_i - [P]_{eq,i})}{V_r}(t_{i+1} - t_i) \quad (27)$$

$$[P]_{eq,i} = \frac{1}{K_A[*]_0}\left(\frac{1}{[P*]_i} - \frac{1}{[*]_0}\right) \quad (28)$$

where Equation (28) is developed using the Langmuir isotherm. The best fit value for the adsorption rate constant, *k*, was calculated by minimizing the sum of the squared residuals between the experimental data and the model calculations.

The best fit values of the adsorption rate constants were 190 L/s for the Macroprep 25Q and 120 L/s for Q Sepharose, consistent with the faster kinetics seen in Figure 10. However, there were large uncertainties in both of these values due to the high degree of scatter between the model and data. This was in large part due to the small number of data points at very short times, the region in which the changes in the liquid and solid-phase concentrations are most dramatic. Figure 11 shows the fit of the model to the experimental data for the adsorption of 3.3 g/L BSA by 15% Q Sepharose.

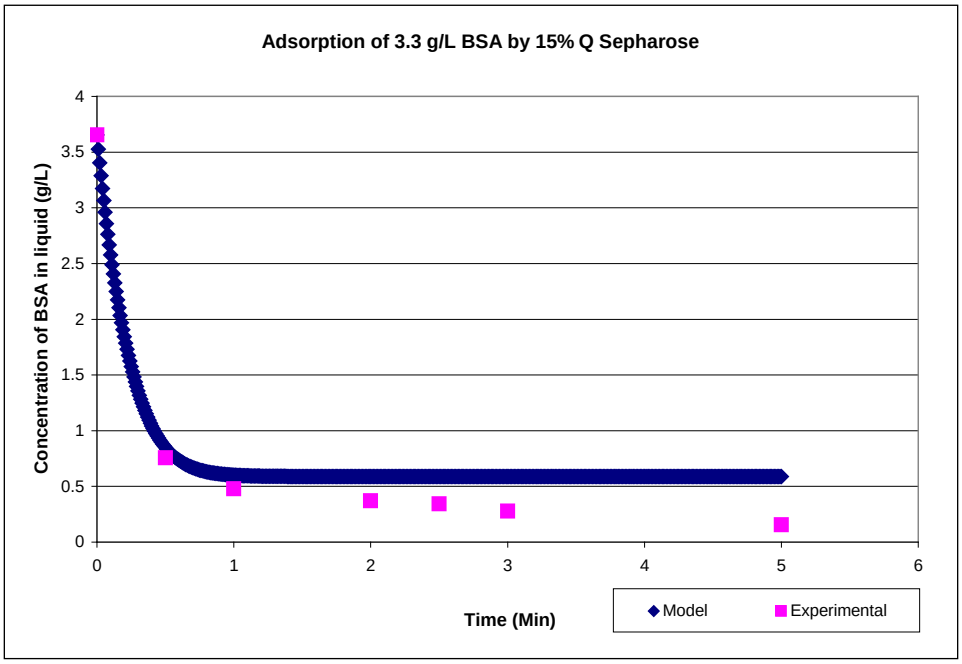

Figure 11: Adsorption kinetics for Q Sepharose with 3.3 g/L BSA in 20 mM PBS, 6.25 mM NaCl at pH 7 with the simple kinetic model

The lumped mass transfer coefficient in the binding model is actually equal to the product of an intrinsic mass transfer coefficient, K_m, and the external surface area, A, of

the resin. The total surface area of the resin can be expressed in terms of the surface area per unit volume, a, of each particle as:

$$k = K_m A = K_m a V_r \tag{29}$$

For uniform spherical particles, the surface area per unit volume is dependent on the particle radius as:

$$a = \frac{4\pi r^2}{4/3 \pi r^3} = \frac{3}{r} \tag{30}$$

This suggests that the intrinsic mass transfer coefficient for BSA adsorption to the Macroprep 25Q is actually smaller than that for Q Sepharose. The reason for this behavior is unclear. If the rate limiting step were the actual binding kinetics, then one might expect the intrinsic binding constants for the two resins to be similar since they both contain a quaternary amine functionality. However, if the adsorption were limited by internal mass transfer within the particle, the Macroprep 25Q should have the greater intrinsic mass transfer coefficient due to its smaller size (and thus smaller diffusional path length). Similarly, if the adsorption were limited by external mass transfer, the intrinsic mass transfer coefficient would again be larger for the Macroprep 25Q due to its smaller size.

The rate of protein desorption is even more rapid than the rate of adsorption as seen in Figure 12 below. Desorption from the Macroprep 25Q was essentially complete within the first 30 s after addition of the high salt concentration buffer. It was not possible to obtain samples more rapidly with the experimental set-up used in this work, making it impossible to calculate the lumped mass transfer coefficient for desorption. Similar results were obtained with the Q Sepharose resin.

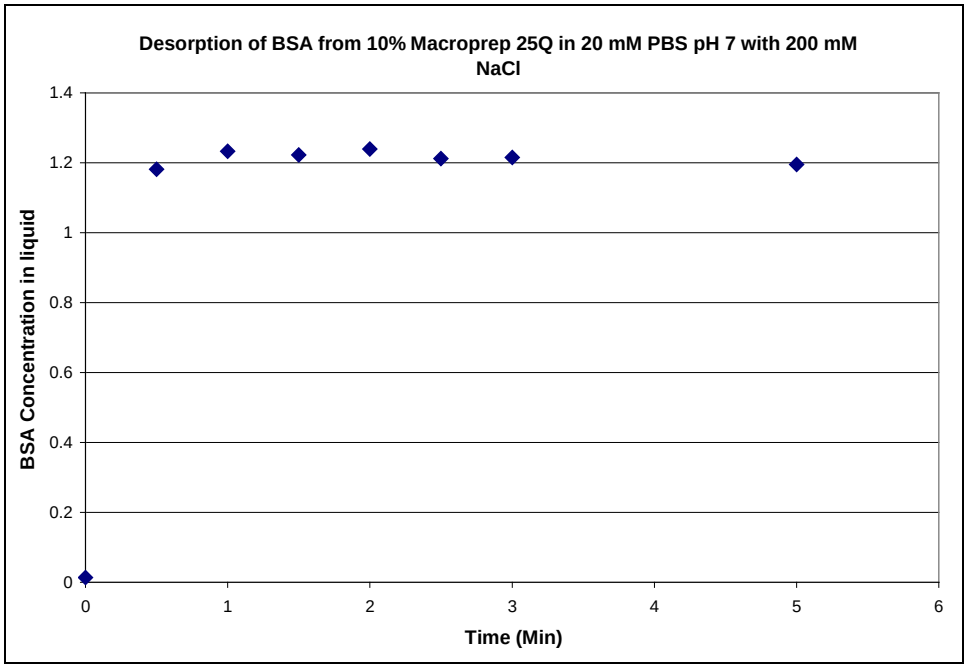

Figure 12: Desorption kinetics for BSA using the Macroprep 25Q in 20 mM PBS pH 7 with 200 mM NaCl

4.5. Myoglobin Adsorption

Figure 13 shows typical results for myoglobin adsorption to the Macroprep 25Q resin. The data were obtained by mixing 7 mL of slurry having a resin concentration of 42% with 33 mL of a myoglobin solution with a concentration of 0.35 g/L. The initial myoglobin concentration in the liquid phase immediately after addition of the slurry can be estimated as 0.31 g/L, assuming that the packed resin actually contains 70% solids. As shown in Figure 4, the Macroprep 25Q shows no myoglobin adsorption, with the myoglobin concentration in the liquid phase remaining constant throughout the experiment. The lack of any myoglobin adsorption is consistent with the repulsive electrostatic interactions between the positively charged myoglobin and the positively

charged Macroprep 25Q. Similar results were obtained for myoglobin adsorption to the Q Sepharose resin under the same experimental conditions.

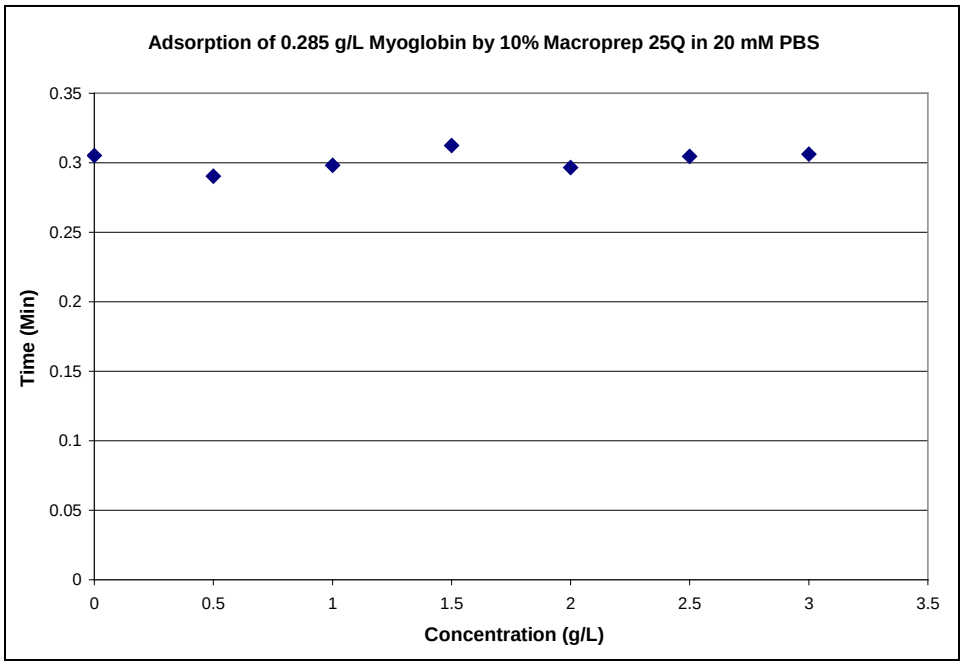

Figure 13: Myoglobin adsorption to the Macroprep 25Q in 20 mM PBS, 6.25 mM NaCl at pH 7. Data obtained with a 0.29 g/L myoglobin and a 10% resin concentration.

5. Conclusions

The experimental studies performed in this thesis were designed to provide information on the equilibrium binding capacity and adsorption / desorption kinetics for a model negatively-charged protein (bovine serum albumin) using 2 different anion exchange resins: the Macroprep 25Q and the Q Sepharose. Equilibrium adsorption data for BSA to the ion exchange chromatography resins were in good agreement with the general form of the Langmuir binding isotherm. The maximum capacity of BSA for the Macroprep 25Q is 13 g/L with an equilibrium constant of 11 L/g compared to values of 35 g/L and 5 L/g for the Q Sepharose. Myoglobin binding was negligible to both resins, consistent with the electrostatic repulsion between the negatively-charged myoglobin and the negatively-charged resin.

Protein desorption from both resins was very rapid, with essentially complete desorption within the first 30 s (less than the time needed to obtain the first sample). Adsorption was somewhat slower, although equilibrium was still obtained within just a few minutes. The calculated values of the lumped mass transfer coefficient for BSA adsorption to the Macroprep 25Q is 190 L/s while that for the Q Sepharose is 120 L/s, consistent with the smaller particle size for the Macroprep 25Q. However, the simple mass transfer model wasn't in particularly good agreement with the experimental data, although this was largely due to the very small number of data points during the initial rapid transient in protein binding. Additional experimental studies using a more rapid sampling method, possibly a stop-flow system, would hopefully provide more quantitative information on the rate of adsorption to the two resins.

The binding data obtained with the Q Sepharose and Macroprep 25Q can be used to guide the design of a countercurrent tangential chromatography system for the separation of a model protein mixture of BSA and myoglobin. The equilibrium binding values can be used to determine the volume of resin needed to obtain high yield of BSA in the capture (binding) step. The adsorption kinetic data can be used to determine the residence time required in the static mixer needed to allow the system to approach equilibrium prior to the filtration in the hollow fiber module. The faster kinetics for the Macroprep 25Q allows one to use a smaller static mixer or to operate the system at a higher flow rate, which would enable the purification of the therapeutic protein in a shorter time.

Future work on countercurrent tangential flow chromatography should examine the binding characteristics of a monoclonal antibody to an affinity Protein A resin. Monoclonal antibodies are the dominant class of protein products in the development pipeline at most biotechnology companies. Protein A is immobilized on a solid support and binds to the Fc (constant) region of IgG. Protein A is currently used as the capture step in the purification of essentially all monoclonal antibody products. Protein A is also the most expensive step in the downstream purification process. The development of an effective countercurrent tangential flow chromatography system, based on appropriate binding results, could potentially provide significant cost savings in the downstream processing of recombinant monoclonal antibody products.

6. References

[1] A. Lyddiatt, Process Chromatography: Current Constrains and Future Options for the Adsorptive Recovery of Bioproducts, *Curr Options in Biotechnol.*, 13 (2002) 95-103.

[2] Y. Yigzaw, P. Hinckley, A. Hewig, and G. Vedantham, Ion Exchange Chromatography of Proteins and Clearance of Aggregates, *Curr Pharm Biotechnol*. 10 (2009) 421-436.

[3] X. Geng and L. Wang, Liquid Chromatography of Recombinant Proteins and Protein Drugs, *J Chromatogr B Analyt Technol Biomed Life Sci.* 15 (2008) 133-153.

[4] A. Velayudhan and M.K. Menon, Modeling of Purification Operation in Biotechnology: Enabling Process Development, Optimization, and Scale-up, *Biotechnol. Prog.* 23 (2007) 68-73.

[5] J. M. Lee, Biochemical Engineering (eBook Version 2.32), Washington State University, Pullman, WA (2009) pp. 322-324.

[6] R. G. Harrison, P. Todd, S. R. Rudge and D. P. Petrides, Bioseparations Science and Engineering, Oxford University Press, New York, (2003) pp. 191-201.

[7] J. C. Bosma and J. A. Wesselingh, pH Dependence of Ion-Exchange Equilibrium of Proteins, *AIChE J.*, 44 (1998) 2399-2409.

[8] E.S. Langer, Trends in Capacity Utilization for therapeutic monoclonal antibody production, *mAbs*., 1 (2009) 151-156.

[9] D. Low, R. O'Leary and N. S. Pujar, Future of Antibody Purification, *J. Chromatogr. B.*, 848 (2007) 43-63.

[10] S. S. Farid, Process Economics of Industrial Monoclonal Antibody Manufacture, *J. Chromatogr. B.,* 848 (2007) 81-18.

[11] O. Shinkazh, Countercurrent Tangential Chromatography Methods, Systems, and Apparatus, US Patent Provisional application US Serial No 61/150,240, (2009).

[12] J.C. Bellot and J. S. Condoret, Modelling of Liquid Chromatography Equilibria, *Proc. Biochem.*, 28 (1993) 365-376.

[13] C. A. Brooks and S. M. Cramer, Steric Mass Action Ion Exchange: Displacement Profiles and Induced Salt Gradients, *AIChE J.* 38 (1992) 1969-1978.

[14] Q Sepharose Fast Flow Instructions, Ed AA, Amersham Biosciences AB.

[15] Macroprep 25 Ion Exchange Supports, Bio-Rad.

[16] A. Staby, I. H. Jensen, and I. Mollerup, Comparison of Chromatographic Ion-Exchange Resins I. Strong Anion Exchange Resins, *J. Chromatogr., A* 897 (2000) 99-111.

Acknowledgements

First and foremost, I would like to thank Dr. Andrew Zydney for all his help, especially during the past year. My experience in lab has taught me so much about planning and executing a long term project. I could not have done any of it without his guidance.

I would also like to thank Oleg Shinkazh for seeing my potential to do research in cooperation with Chromatan, Inc. His guidance, especially in the beginning, really helped me learn to designing experiments and understand the importance of the project.

I would like to thank Dharmesh and all the other grad students for being extremely helpful whenever I needed anything. Their patience and explanations taught me so much over the past year.

I would like to thank Matt Long and my fellow undergraduate researchers for making lab an enjoyable environment. It was a pleasure working side-by-side with all of them.

I would like to thank my family and friends for their support throughout the writing of this thesis. Researching in lab and writing the actual report was a huge time commitment and my family and friends were always supportive of the time I was required to devote and encouraging whenever I got discouraged. I would particularly like to thank my roommate, Lindsey Earle. Her support and encouragement kept me motivated and optimistic throughout a very stressful year.

Academic Vita of Morgan Barth

Education

B.S. Chemical Engineering, Bioprocess and Biomolecular Engineering Option
The Pennsylvania State University, Schreyer Honors College

Work Experience

Process Research & Development intern, Genentech, Inc (Summer 2009)
Process Improvement Intern, Ortho Clinical Diagnostics, a J&J company (Spring and Summer 2008)

Awards & Scholarships

Academic Excellence Scholarship (Fall 2006 – Spring 2010)
Beier Engineering Scholarship (Fall 2007 – Spring 2010)
President's Freshman Award (2007)
Dean's List (Fall 2006 – Fall 2009)
Encore Award, Ortho Clinical Diagnostics (Summer 2008)
PR&D Award and Scholarship, Genentech, Inc. (Fall 2009 – Spring 2010)

Leadership

Supply Logistics Captain, Penn State IFC/Panhellenic Dance Marathon (2010)
Cross-Country Club Dancer, Penn State IFC/Panhellenic Dance Marathon (2009)
Vice-president, Cross-Country Club, (2009)
Vice-president, Triathlon Club (2008-2009)